RhoGEF2 and the formin Dia control the formation of the furrow canal by directed actin assembly during *Drosophila* cellularisation

Jörg Großhans[1,*,†], Christian Wenzl[1,*], Hans-Martin Herz[1], Slawomir Bartoszewski[1], Frank Schnorrer[2], Nina Vogt[2], Heinz Schwarz[2] and H.-Arno Müller[3]

[1]ZMBH, Universität Heidelberg, Im Neuenheimer Feld 282, 69120 Heidelberg, Germany
[2]Max-Planck-Institut für Entwicklungsbiologie, Spemannstraße 35, 72076 Tübingen, Germany
[3]Institut für Genetik, Heinrich-Heine-Universität Düsseldorf, Universitätsstrasse 1 Geb. 26.02., 40225 Düsseldorf, Germany
*These authors contributed equally to this work
†Author for correspondence (e-mail: j.grosshans@zmbh.uni-heidelberg.de)

Development 132, 1009-1020
Published by The Company of Biologists 2005
doi:10.1242/dev.01669

Accepted 24 December 2004

Summary

The physical interaction of the plasma membrane with the associated cortical cytoskeleton is important in many morphogenetic processes during development. At the end of the syncytial blastoderm of *Drosophila* the plasma membrane begins to fold in and forms the furrow canals in a regular hexagonal pattern. Every furrow canal leads the invagination of membrane between adjacent nuclei. Concomitantly with furrow canal formation, actin filaments are assembled at the furrow canal. It is not known how the regular pattern of membrane invagination and the morphology of the furrow canal is determined and whether actin filaments are important for furrow canal formation. We show that both the guanyl-nucleotide exchange factor RhoGEF2 and the formin Diaphanous (Dia) are required for furrow canal formation. In embryos from *RhoGEF2* or *dia* germline clones, furrow canals do not form at all or are considerably enlarged and contain cytoplasmic blebs. Both Dia and RhoGEF2 proteins are localised at the invagination site prior to formation of the furrow canal. Whereas they localise independently of F-actin, Dia localisation requires *RhoGEF2*. The amount of F-actin at the furrow canal is reduced in *dia* and *RhoGEF2* mutants, suggesting that RhoGEF2 and Dia are necessary for the correct assembly of actin filaments at the forming furrow canal. Biochemical analysis shows that Rho1 interacts with both RhoGEF2 and Dia, and that Dia nucleates actin filaments. Our results support a model in which *RhoGEF2* and *dia* control position, shape and stability of the forming furrow canal by spatially restricted assembly of actin filaments required for the proper infolding of the plasma membrane.

Key words: formin, blastoderm, furrow canal, morphogenesis, *Drosophila melanogaster*

Introduction

Many morphogenetic processes during development involve precise changes in the shape of the plasma membrane. Migrating cells form extensions at their leading edge, while during cytokinesis the plasma membrane constricts between the future daughter cells (Glotzer, 2001). The curvature of the plasma membrane is determined to a large degree by the cortical cytoskeleton with actin filaments being an integral part of it (Revenu et al., 2004). Shape changes and internalisation events require a reorganisation of the cell cortex and the actin cytoskeleton, which is controlled by GTPases of the Rho family (Etienne-Manneville and Hall, 2002; Lu and Settleman, 1999a).

The enclosure of the nuclei into cells during the cellular blastoderm of *Drosophila* embryos is achieved by a specialised process of membrane invagination and reorganisation of the actin cytoskeleton (Foe et al., 1993; Schejter and Wieschaus, 1993; Mazumdar and Mazumdar, 2002). Following the exit from the last mitosis of the cleavage stage, the plasma membrane folds in between adjacent nuclei to form the furrow canals that are visible by light microscopy as the cellularisation front after about 10 to 20 minutes when the shape of the nuclei is already ellipsoid. The furrow canals have a diameter of about 0.2 μm, are coated with actin filaments and remain connected with the surface plasma membrane. Apical to the furrow canal the so-called basal junction tethers the two adjacent membranes and thus stabilises the furrow (Hunter and Wieschaus, 2000). The mechanism of the spatially restricted assembly of F-actin at the furrow canal, as well as the factors that nucleate F-actin at this site, have not yet been identified. Furthermore, it is unclear whether actin filaments have an instructive function for the initial formation and shape of the furrow canal.

A few genes are known to be involved in furrow canal formation. Embryos mutant for *nullo*, *sry*-α, *nuf*, *Rab11*, *Abl*, *dah* or *dia* lack furrow canals between adjacent nuclei to a variable extent, which leads to the formation of multinuclear cells (Schweisguth et al., 1990; Postner and Wieschaus, 1994; Zhang et al., 1996; Rothwell et al., 1998; Afshar et al., 2000; Riggs et al., 2003; Grevengoed et al., 2003). Among this group of genes, *nullo* and *sry*-α are particularly interesting because they are early markers for the furrow canal and affect the formation of the basal junction (Hunter and Wieschaus, 2000). Another early marker for the furrow canal is the novel protein

Slam, which is required for timed invagination of the furrow. Localised to the furrow canal and the basal junction, Slam recruits MyoII to the furrow canal and affects the accumulation of Arm at the basal junction (Lecuit et al., 2001; Stein et al., 2002). However, a direct link to furrow canal formation and F-actin polymerisation has not been established for any of the genes in this group.

To identify additional components required for proper cell morphology in the blastoderm we have screened a large collection of female-sterile mutants derived from germline clones (Luschnig et al., 2004) (our unpublished data). We found two allelic mutations that affect the cellularisation front. Mapping and complementation analysis identified *RhoGEF2* as the mutated gene.

RhoGEF2 is required during gastrulation for apical constriction of the cells undergoing mesoderm invagination (Barrett et al., 1997; Häcker and Perrimon, 1998). Although there is evidence that RhoGEF2 genetically interacts with Rho1 and is controlled by Folded gastrulation during *Drosophila* gastrulation, the mechanism of how *RhoGEF2* controls cell shape at this stage and whether this involves spatially restricted control of F-actin is not understood.

Potential effectors of RhoGEF2 and Rho1 are Rho kinase/sqh/myoII (Royou et al., 2004), citron kinase (Shandala et al., 2004; Naim et al., 2004; D'Avino et al., 2004), protein kinase N (Lu and Settleman, 1999b) and Diaphanous (Dia). As there are no indications that Rho kinase/sqh/myoII and citron kinase would have a similar function for furrow canal formation as RhoGEF2, we concentrated in our analysis on *dia*, which is a member of the protein family with formin-homology domains (FH) that control formation of actin filaments (Wallar and Alberts, 2003). Biochemical and structural studies of the yeast (BNI1) and mouse (mDia; also known as Diap1 – Mouse Genome Informatics) homologues have shown how actin filaments are nucleated (Pruyne et al., 2002; Sagot et al., 2002; Li and Higgs, 2003; Xu et al., 2004; Shimada et al., 2004; Higashida et al., 2004; Romero et al., 2004). mDia1 is assumed to be activated by binding of Rho1 that releases an inhibitory intramolecular interaction of the C-and N-terminal domains of mDia1 (Alberts, 2001; Watanabe et al., 1997; Watanabe et al., 1999). However, this activation mechanism could only partially be reconstituted in vitro (Li and Higgs, 2003). Besides controlling actin fibres, Dia may also regulate microtubules (Ishizaki et al., 2001; Palazzo et al., 2001; Wen et al., 2004; Yasuda et al., 2004). On a physiological level, the function of Dia and formins are less defined. The M-formin1 may link actin filaments to adherence junctions by an interaction with α-catenin (Kobielak et al., 2004), and mDia3 may regulate attachment of microtubules to kinetochores during mitosis (Yasuda et al., 2004). In *Drosophila dia* is required for cytokinesis in the male germline, formation of pole cells and pseudo cleavage furrows during embryonic cleavage stage (Castrillon and Wasserman, 1994; Afshar et al., 2000). Furthermore cellularising embryos from *dia* germline clones have defects in the arrangement and cortical connection of the nuclei (Afshar et al., 2000). During this stage Dia protein localises to the furrow (Afshar et al., 2000), which makes it a good candidate for controlling spatially restricted actin polymerisation at the furrow canal. However, the site of Dia protein localisation has neither been defined in detail nor correlated to the morphological defects of the mutant.

We describe here a new function of *RhoGEF2* and *dia* in the formation of the furrow canal. Mutant embryos have strongly enlarged furrow canals containing cytoplasmic blebs. Double immunolabelling studies show that RhoGEF2 and Dia are specifically concentrated between adjacent nuclei before the cellularisation front becomes visible and thus may serve as a template for the hexagonal pattern of membrane invagination. The amount of F-actin at the furrow canal is reduced in *RhoGEF2* and *dia* mutants, suggesting that RhoGEF2 and Dia assemble actin filaments at the site of invagination and thus control the location, size and stability of the furrow canal. This further implies that spatially restricted F-actin polymerisation plays an important role for the initial infolding of the plasma membrane. Since many furrow canals still form in the absence of *RhoGEF2* or *dia*, we tested whether *nullo* has a redundant function. Embryos lacking both *RhoGEF2* and *nullo*, as well as embryos lacking both *dia* and *nullo*, do not form any furrow canals. This additive effect indicates that *nullo* functions in a genetic pathway separate from *RhoGEF2* and *dia*. We propose that these pathways work in parallel to control two distinct but complementary aspects of furrow canal formation: actin polymerisation at the site of the infolding membrane and adherens junction formation.

Materials and methods

Genetics

Commonly used procedures were applied according to standard protocols (Roberts, 1998) and genetic material and fly strains were as described by FlyBase (http://www.flybase.net). The following chromosomes and alleles were used: Frt^{2R}*RhoGEF2*$^{1.1}$, Frt^{2R}*RhoGEF2*$^{4.1}$ (Barrett et al., 1997), Frt^{2R}*RhoGEF2*^{04291} (Häcker and Perrimon, 1998), *dia*^{5} Frt^{2L} (Afshar et al., 2000), *slam*$^{35.16}$ Frt^{2L} (Stein et al., 2002), Df(3R)X3F (*sry-α*), Df(1)6F (*nullo*), nullo-HA [nullo fused to a haemagglutinin tag and expressed with the *nullo* promoter (Hunter and Wieschaus, 2000)], CyO, *hb-lacZ*, moesin-GFP [line sGMCA-n2 (Kiehart et al., 2000)]. *slam* embryos from *slam* germline clones were identified by absence of the *hb-lacZ* reporter. Germline clones were produced with Flipase-induced mitotic recombination and counter-selection by *ovo*^{D}.

The lethality on chromosome *fs*(2R)201 was fine-mapped to 53EF by meiotic recombination with the w^{+} of P-element insertions (*l(2)*k03609, *l(2)*k04222b, *l(2)*k07805b). The lethality of the two mutations from our screen, *fs*(2R)201 and *fs*(2R)350 was not complemented by the previously identified *RhoGEF2*$^{1.1}$ (Barrett et al., 1997). As the transcript is missing in the allele *RhoGEF2*^{04291}, the described defects most probably represent a complete loss-of-function phenotype (Häcker and Perrimon, 1988). The *RhoGEF2* phenotype (allele fs(2R)201), as well as the *dia* phenotype depend only on the maternal genotype, because zygotically homozygous and heterozygous embryos, as marked with a *hb-lacZ* reporter gene showed the same range of defects (data not shown). Molecular characterisation of the *dia*^{5} locus showed that about 3 kb of the original P element remained at the original insertion site (data not shown).

Histology

Embryos were heat-fixed in 0.4% NaCl, 0.03% Triton X-100 or fixed with 4% formaldehyde in PBS (except for phalloidin staining when 8% formaldehyde was used) and stored in methanol. Fixed embryos were stained in PBS with 0.2% Triton X-100 consecutively with solutions of primary antibody, fluorescent secondary antibodies (4 μg/ml, Alexa488, Alexa546, Alexa647; Molecular Probes), DNA dyes (DAPI, Hoechst, Oligreen or propidium iodide) and mounted in

either Mowiol/DABCO or Aquapolymount (Polyscience). Antibodies to the following proteins were used: RhoGEF2 (0.1 μg/ml), Dia (1:4000; J. G. and S. Wasserman), Slam [1:5000 (Stein et al., 2002)], MyoII (B. Mechler), Arm (1:50), Sry-α (1:10), Dlg (1:20; Hybridoma Center), HA (12CA5, 1 μg/ml; Roche), β-gal (0.1 μg/ml; Roche), γ-tubulin (0.2 μg/ml; Sigma), phalloidin coupled to Alexa dyes (6 nM; Molecular Probes). To compare Dia and F-actin distribution in wild-type, *RhoGEF2* and *dia* embryos, embryos of the two genotypes to be compared were mixed prior to fixation and processed as a mixture. Wild-type embryos were marked with a nullo-HA transgene, by the presence of RhoGEF2 staining or recognised by a proper F-actin array. For quantification of the *RhoGEF2* or *dia* mutant phenotype nuclei in fields of 238×238 μm were counted in embryos stained with either Arm or Dlg antibodies or phalloidin.

Microscopy

Fluorescent images were recorded with a Leica confocal microscope (DMIRE2, 20× NA 0.7 water, HCX PL APO 63× NA1.2 corr, HCX PL APO 63× NA1.4-0.6 oil, laser at 405, 488, 543, 633 nm). Development of live embryos was recorded using an inverted microscope with differential interference contrast optics and a computer controlled stage (Leica DMIRE2, PL APO 63× NA1.4-0.6 oil; Hamamatsu ORCA-ER, Openlab software, Improvision). Digital photographs were processed with Photoshop (Adobe). For the analysis of the ultrastructure, embryos were staged in halocarbon oil (27S, Sigma) with a dissecting microscope. After removing the chorion with hypochlorite and rinsing, embryos were transferred to hexadecen, mounted in 100 μm deep aluminium plates and fixed by rapid high pressure freezing using a Balzer HPFM 10 machine. Fixed embryos were collected in liquid nitrogen and freeze-substitution was carried out with acetone containing 2% OsO_4 at –90°C for 24 hours, –60°C for 6 hours and –40°C for 3 to 9 hours. Following embedding in Epon, sectioning and staining with Pb(II)citrate and U(II)acetate, specimens were examined on a Zeiss 109 or Philips CM10 transmission electron microscope.

Microinjection, drug treatment

Eggs were dechorionated in 50% bleach, dried in a desiccation chamber, covered with halocarbon oil and subsequently injected posteriorly with 50-100 pl of aqueous dsRNA at 1 μg/μl except for *sry-α* dsRNA, which was injected into wild-type embryos at 6 μg/μl. Embryos were fixed with 4% formaldehyde for 30 minutes. The vitelline membrane was removed manually. For the latrunculin A treatment, dechorionated embryos were incubated for 2.5 minutes in *n*-heptane to permeabilise the vitelline membrane, briefly rinsed in PBT (PBS plus 0.1% Tween 20), incubated for 6 minutes at room temperature in PBS containing 50 μg/ml latrunculin A (P. Crews, Santa Cruz, USA) and subsequently fixed in formaldehyde.

Molecular genetics

DNA encoding indicated fragments were amplified by PCR, cut by appropriate restriction enzymes and cloned into the indicated vectors: RhoGEF2 (aa1-687)-His_6, as a *Nco*I-*Bgl*II into pQE80N60 (Görlich), GST-RhoGEF2 (aa1512-1897), *Eco*RI-*Sal*I into pGEX-4T-1 (Pharmacia). Dia aa 1-464 (pCS-diaΔC464) as *Sal*I-*Xba*I into pCS2 (R. Rupp, Munich). Dia aa 318-1091 (pCS-diaΔN318) as *Sal*I-*Xba*I into pCS2. ZZ-dia-His_6 fusions: Dia aa 1-518 (pZZ-diaΔC518) or Dia aa 519-1091 (pZZ-diaΔN519), *Kpn*I-*Sal*I into pQE80ZZ (Görlich). The point mutations T1544A (codon1544 mutated to GCT) in the GEF domain of RhoGEF2 and the Rho1Q63L (codon 63 mutated to CTG) were introduced by inverse PCR with Pfu polymerase (Stratagene). GST fusion constructs of RhoA, RhoL, Cdc42, Rac1, Rac2, Mtl1 and the TrioGEF-D1 are described previously (Newsome et al., 2000). DNA templates for the synthesis of dsRNA were amplified with a T7 promoter site at their ends (*nullo* 586 bp, *sry-α* 568 bp, Bsg25D 561 bp). Respective dsRNA fragments were synthesised with T7 RNA polymerase (Ambion MEGAscript). Details are available upon request.

Biochemistry

Purification of GST fusion proteins

E. coli BL21DE expressing the fusion proteins from pGEX plasmids were lysed in 50 mM Tris-HCl pH 8, 100 mM NaCl, 10 mM $MgCl_2$, 1 mM DTT, 1 mM PMSF in a French press. GST fusion proteins were purified from the soluble fraction by GSH affinity chromatography (GSTrapFF, Amersham; wash buffer 50 mM Tris-HCl pH 8, 500 mM NaCl, 10 mM $MgCl_2$, 1 mM DTT, elution buffer 50 mM Tris-HCl pH 8, 50 mM NaCl, 10 mM glutathione, 1 mM DTT), dialysed against 50 mM Tris-HCl pH 7.5, 50 mM NaCl, 10 mM MgCl, 1 mM DTT, 10% glycerol and stored in aliquots at –80°C with an additional 250 mM saccharose.

Purification of His-tagged proteins

Native or denatured extracts from *E. coli* BL21DE were purified by nickel chelate chromatography (Ni NTA agarose, Qiagen).

Immunisation

Rabbits or guinea pigs were immunised with a denatured N-terminal fragment of RhoGEF2 (aa 1-687) or native ZZ-diaΔN519. Antibodies were purified by affinity chromatography with Sepharose (BrCN activated Sepharose; Pharmacia, 2.5 ml) with coupled RhoGEF2 (aa 1-687+H_6, 10 mg, native). Antibodies were eluted with 50 mM glycine pH 3.5, dialysed against PBS and concentrated.

Guanyl-nucleotide exchange assay

GTPase (0.2 μM) loaded with [8-^{3}H]GDP (426 GBq/mmol; Amersham) and 0.1 μM of the corresponding GEF were incubated at 25°C for 20 minutes, or as indicated. After nitrocellulose filtration, the radioactivity on the filter was determined in a liquid scintillation counter. The assay was performed in duplicate (Debant et al., 1996) (S. Schmidt, Montpellier, France).

For western blot analysis, extracts of approximately 50 embryos were separated on SDS-PAGE and transferred by semi-dry blotting to a nitrocellulose membrane (Schleicher and Schuell). Antibodies were diluted as follows: Dia 1:5000, Dlg 1:100, RhoGEF2 1:20000, β-tubulin 1:10000. The blots were developed with IgG coupled with peroxidase and chemiluminescence (ECLplus, Amersham, Kodak X-OMAT).

For radioactive labelling, proteins were expressed from template plasmids carrying a modified β-globin leader sequence (pCS2 derivatives) with SP6 RNA polymerase in a coupled in vitro transcription-translation system (TNT, Amersham) supplemented with [^{35}S]methionine (37 TBq/mmol; Amersham).

Binding assay

10 μl of GSH-Sepharose (Pharmacia) loaded with approximately 10 μg GST fusion proteins were incubated with 2 μl of labelled protein in 400 μl binding buffer (50 mM Tris-HCl pH 7.5, 300 mM NaCl, 1 mM DTT, 10 mM $MgCl_2$, 0.2% Tween) for 1 hour at 4°C. After washing six times with binding buffer, proteins were eluted with 2×50 μl of 10 mM glutathione, 50 mM Tris-HCl pH 7.5, 50 mM NaCl, 1 mM DTT, 10 mM $MgCl_2$, 0.2% Tween and precipitated with 5% TCA. Following SDS-PAGE the label was visualised with a phosphoimager (Fuji BAS1000).

Actin polymerisation assay

The indicated protein solution (60 μl) in G-buffer (20 μM $CaCl_2$, 20 μM ATP, 0.5 mM Tris-HCl pH 8) and 10 μl of polymerisation buffer (12.5 mM KCl, 0.5 mM MgCl2, 25 μM ATP) were added to 30 μl of G-actin (10% labelled with pyrene, final concentration 3 μM; Cytoskeleton, USA). Fluorescence was excited at 365 nm and recorded at 407 nm.

Results

RhoGEF2 and *dia* are involved in furrow canal formation

The lethality of the mutation *fs*(2R)201 from our screen of germline clone mutations was mapped to the *RhoGEF2* region by meiotic recombination. Complementation analysis with previously identified alleles showed that it was a new allele of *RhoGEF2* (Barrett et al., 1997; Häcker and Perrimon, 1998). In living embryos from *RhoGEF2* germline clones the cellularisation front was invisible by light microscopy and the nuclei became irregularly arranged during the second half of cellularisation (see Movies 1 and 2 in the supplementary material). Similarly, we observed that in about one half of the embryos from *dia* germline clones (8 out of 14) the cellularisation front was invisible as well (see Movie 3 in the supplementary material). Thus the mutant phenotypes revealed a novel function of *RhoGEF2* and *dia* during cellularisation that had not been described previously.

To investigate possible morphological defects, we analysed the ultrastructure of the furrow canals in embryos during mid-cellularisation by transmission electron microscopy. In wild-type embryos, the furrow canal can be seen as a hairpin loop with a diameter of about 0.2 μm in specimens fixed by high pressure freezing (Fig. 1A,B). Sometimes the diameter of furrow canals appears enlarged because of the plane of the section, in particular at the intersections of furrow canals. In six different embryos from two preparations, we found that 90% of furrow canals had the typical compact loop structure. In contrast, in embryos from *RhoGEF2* germline clones, the furrow canal diameters were enlarged up to three fold and in most cases (78% in 6 embryos examined) did not show the typical hairpin loop (Fig. 1C,D). Instead, cytoplasmic blebs of variable size were present in the furrow canal, which we did not observe in wild-type embryos, suggesting that the enlarged mutant furrow canals are less stable, possibly because of their larger size or changed properties of the membrane. Defects in the morphology of the furrow canals were also observed in embryos from *dia* germline clones. The furrow canals in these embryos were more variable than in *RhoGEF2* mutants ranging from about threefold dilated to diameters of more than 1 μm (Fig. 1E,F). Based on the analysis of the ultrastructure we conclude that *RhoGEF2* and *dia* are required for compact and stable furrow canals during cellularisation.

Furthermore, in embryos from *RhoGEF2* and *dia* germline clones furrow canals are not only enlarged, but are often missing between adjacent nuclei. We visualised this aspect of the phenotype by staining for F-actin, which marks the furrow canal and thus a regular hexagonal array is evident in surface views (Fig. 2A). In embryos from *RhoGEF2* and *dia* germline clones these hexagons were frequently interrupted (Fig. 2B,D) and a variable proportion of the forming cells contained multiple nuclei (Fig. 2F,G). In contrast, the hexagonal array was complete in embryos mutant for *slam* (Fig. 2E), suggesting that *slam* controls different aspects of furrow canal formation than *RhoGEF2*, *dia* and *nullo*. The proportion of multinuclear cells was not different in embryos early or late in cellularisation, indicating that the defect occurs during the formation of the furrow canal. In about half of the embryos from *dia* germline clones almost all cells contained multiple nuclei, which is consistent with the variable and often severely disturbed morphology of these embryos (Fig. 2G).

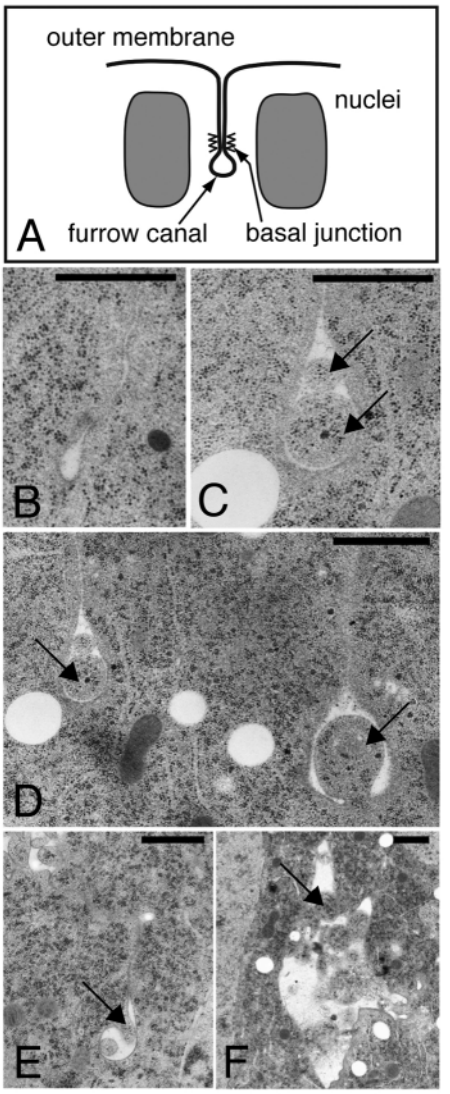

Fig. 1. Dilated furrow canals in embryos from *RhoGEF2* and *dia* germline clones. (A) Schematic drawing of cellularisation showing the furrow canal, basal junction and plasma membrane. Embryos prepared for TEM by high pressure freezing and freeze substitution. (B) In the wild-type embryo, furrow canals are seen as a dilatation of the plasma membrane growing in from the apical surface. In embryos from (C,D) $RhoGEF2^{1.1}$ and (E,F) *dia* germline clones, furrow canals are considerably enlarged and filled with large cytoplasmic blebs (arrows in C,D,E). No simple hairpin structure can be seen in most of the cases. Apical side up. Scale bars: 0.5 μm.

To confirm the specificity of the defects in furrow canal formation, we checked whether other aspects of cellularisation, membrane invagination, nuclear extension and basal closure are affected. Membrane invagination and nuclear extension were compared in embryos from *RhoGEF2* germline clones (n=10) and wild-type (n=5) embryos by time-lapse recordings (see Movies 1 and 2 in the supplementary material). For both genotypes, the nuclei extended at the same rate and cellularisation was completed in about 60 minutes (T=20–22°C). Staining of the furrow canal with Slam antibodies (Stein et al., 2002) showed a widening and pinching off of the base of the furrow canal, which indicates that basal closure occurs (see Fig. S1 in the supplementary material).

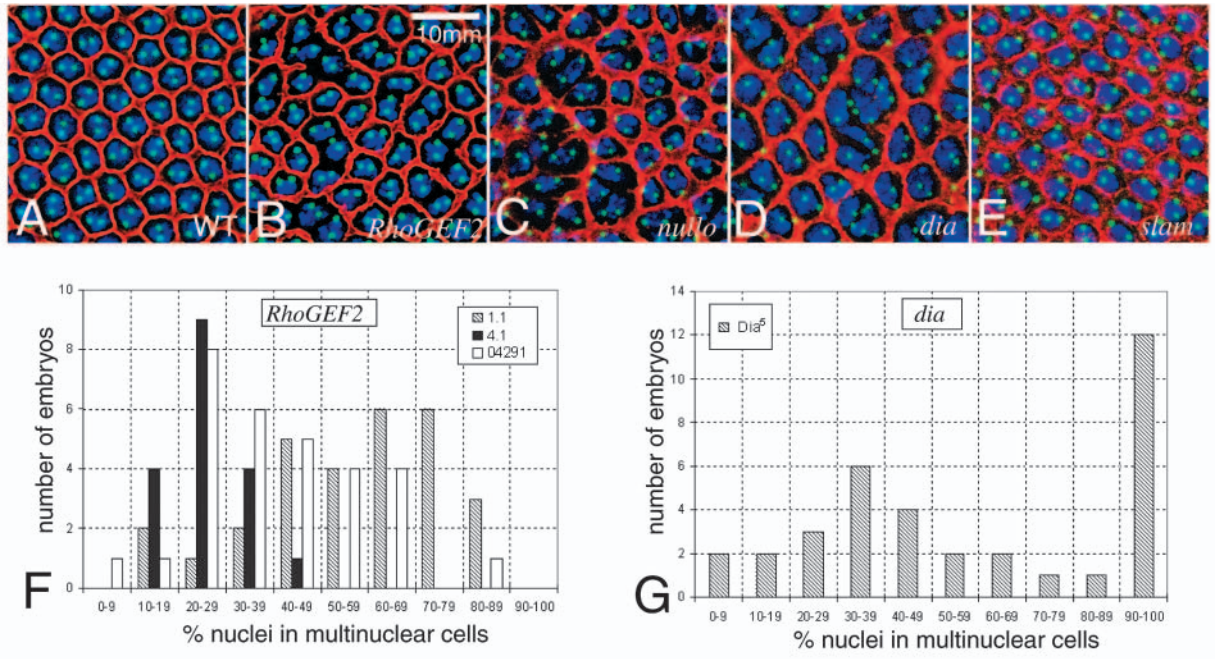

Fig. 2. Multinuclear cells in embryos from *RhoGEF2* and *dia* germline clones. (A-E) Embryos of the following genetic constitution were stained for DNA (blue), γ-tubulin (green, added from a higher optical section) and F-actin (red). (A) Wild type, (B) from *RhoGEF2*$^{1.1}$ germline clones, (C) *nullo*, (D) from *dia* germline clones and (E) *slam* embryos from *slam* germline clones. Number of embryos with indicated proportion of nuclei in multinuclear cells plotted for (F) *RhoGEF2* alleles (1.1, 4.1, 04291) and for (G) *dia*. Scale bars: 10 μm.

These data show that *RhoGEF2* does not play a significant role in membrane invagination, basal closure and nuclear elongation and that even the dilated and abnormal furrow canals can lead the invagination of the plasma membrane at normal speed. The morphology in embryos from *dia* germline clones was more disturbed and variable (Afshar et al., 2000), especially in later cellularisation, the plasma membrane invaginates, possibly with a delay and indications of basal closure were clearly observed at least in some embryos (see Movie 3 and Fig. S1 in the supplementary material).

Distinct functions of *RhoGEF2* and *nullo* in furrow canal formation

nullo and *sry-α* are also required for correct furrow canal formation (Postner and Wieschaus, 1994; Schweisguth et al., 1990). *nullo* and *sry-α* mutant embryos contain multinucleate cells because furrow canals are frequently absent (Fig. 2C). *sry-α* probably acts downstream of *nullo*, because Sry-α protein localisation depends on *nullo* (Postner and Wieschaus, 1994). To test whether they act in the same genetic pathway as *RhoGEF2* or *dia*, we analysed the formation of the furrow canals, marked by F-actin in embryos lacking both gene functions by producing RNAi-induced phenocopies of *nullo* or *sry-α* in embryos from *RhoGEF2* or *dia* germline clones (Fig. 3; see Fig. S2 in the supplementary material). In embryos from *RhoGEF2* germline clones treated with RNAi for *nullo* (73%, *n*=33, Fig. 3B,E) or *sry-α* (63%, *n*=16, Fig. 3C,D), F-actin at the furrow canal was almost absent and only a few singular rings and irregular patches remained. The strength of the 'double mutant' phenotype directly correlated with the amount of Sry-α protein as seen in embryos with locally deposited *sry-α* dsRNA at the posterior pole (Fig. 3C). In transversal sections, F-actin staining at the furrow canal was observed only in anterior regions. This staining was gradually lost towards posterior regions in the 'double mutant' situation, which suggests that furrow canals are completely absent (Fig. 3D,E). Following *nullo* or *sry-α* RNAi injection into embryos from *dia* germline clones we observed, in both cases, an almost complete absence of furrow canals (data not shown).

The observed defects are specific because injection of *nullo* or *sry-α* dsRNA into wild-type embryos induced their respective phenocopies (see Fig. S2 in the supplementary material), whereas injection of an unrelated dsRNA did not change the *RhoGEF2* and *dia* mutant phenotypes (Fig. 3A). In contrast to the strongly enhanced phenotype of the *RhoGEF2* – *nullo* 'double mutant', we observed an only slightly enhanced phenotype, when *sry-α* dsRNA was injected into *nullo* embryos (data not shown), which is consistent with the model that *nullo* and *sry-a* act in the same genetic pathway. Since the related phenotypes of *RhoGEF2* and *nullo/sry-α* are additive and since the *RhoGEF2* allele does not form a transcript and the *nullo* and *sry-α* dsRNA induces phenocopies of *nullo* and *sry-α* deficiencies, we conclude that *RhoGEF2* and *nullo/sry-α* function in separate, parallel genetic pathways, suggesting that they control different aspects of furrow canal formation. Injection of *nullo* or *sry-α* dsRNA into embryos from *dia* germline clones leads to lack of F-actin at the furrow canal. Although the similarity of the 'double mutants' with *dia* suggests that *dia* also acts in parallel to *nullo*, a strong conclusion cannot be drawn because it is not clear whether the used *dia* allele is amorphic.

RhoGEF2, Dia and F-actin colocalise at the furrow canal

Dia protein is localised at the furrow (Afshar et al., 2000), whereas the distribution of RhoGEF2 protein has not yet been

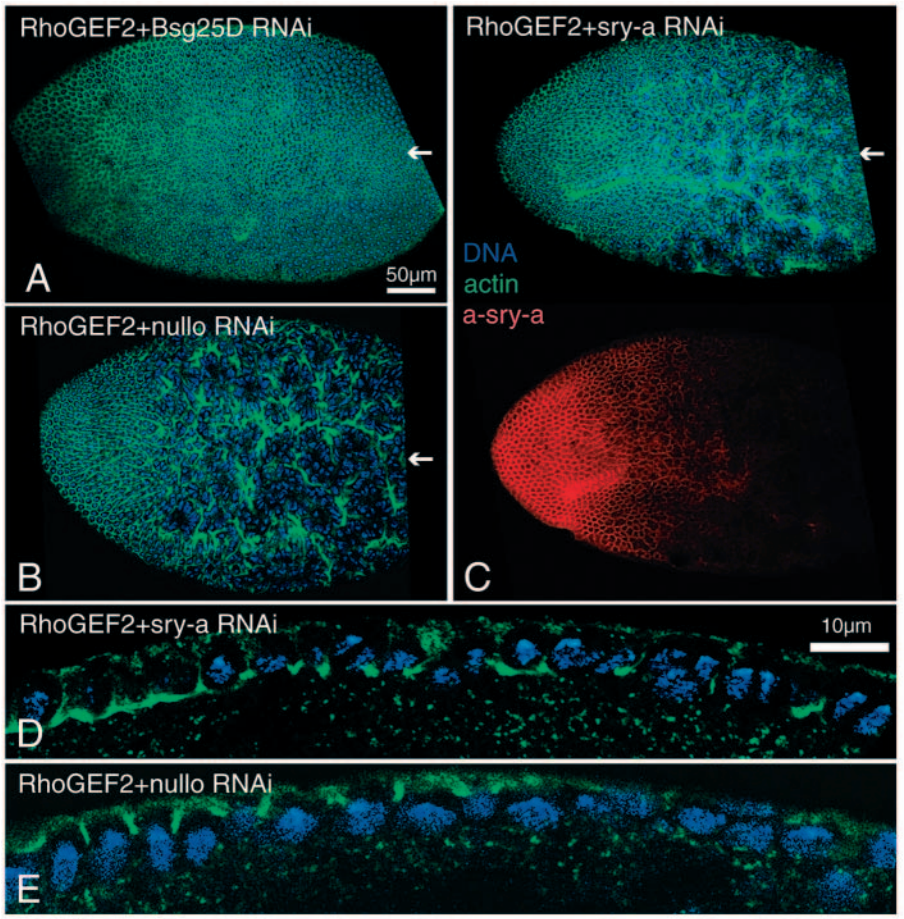

Fig. 3. *RhoGEF2* and *nullo/sry-α* cooperate in furrow canal formation. (A-E) Embryos from $RhoGEF2^{1.1}$ germline clones were injected at the posterior pole with the following dsRNA: (A) *Bsg25D*, (B,E) *nullo*, (C,D) *sry-α*, and stained for DNA (blue), F-actin (green), Sry-α (red). Loss of Sry-α protein and loss of furrow canals (marked by F-actin, optical transversal sections, D,E) correlates with the posterior site of dsRNA injection as shown by respective antibody staining (C). Scale bars: (A-C) 50 μm, (D,E) 10 μm. Posterior to the right, arrow indicates injection site.

determined. We raised antibodies against an N-terminal RhoGEF2 fragment to investigate the intracellular distribution of RhoGEF2. The antibody specifically detects RhoGEF2 because in western blots a band migrating at more than 200 kDa was detected in extracts of wild-type but not of mutant embryos (Fig. 4G). In whole-mount staining of germline clone embryos from four alleles of *RhoGEF2* ($RhoGEF2^{201}$, $RhoGEF2^{1.1}$, $RhoGEF2^{4.1}$, $RhoGEF2^{04291}$) only a low and uniform signal was detected (Fig. 4D), whereas a locally restricted staining was observed at the tip of the furrow throughout cellularisation in wild-type embryos (Fig. 4A-C). The specific staining was visible when the nuclei were still spherical, that is before the cellularisation front appeared. In surface view RhoGEF2 formed a hexagonal array enclosing the nuclei (Fig. 4E). This distribution changed at the onset of gastrulation when RhoGEF2 staining was lost basally in the invaginating ventral cells and simultaneously appeared apically (Fig. 4F). These data show that RhoGEF2 localisation precedes furrow canal formation at the site of invagination, suggesting that it may determine the hexagonal pattern of membrane invagination.

To compare the localisation of RhoGEF2 with Dia, F-actin and Arm and to define the localisation of Dia in detail, we performed multiple immunolabelling. Although the actual formation of the furrow canals occurs within the first phase of cellularisation, we analysed the protein distribution slightly later, when membrane domains can be better distinguished, assuming that the later localisation pattern reflects an intrinsic property of the proteins. RhoGEF2 primarily localises to the furrow canal and not to the basal junction, marked by Arm, since we observed no significant overlap of RhoGEF2 and Arm staining (Fig. 5A). In contrast, RhoGEF2, Dia and F-actin staining clearly matched each other, and therefore colocalise at the furrow canal (Fig. 5C-E). As in the case of RhoGEF2, Dia localisation appears to precede furrow canal formation, since the specific staining was already observed when the nuclei were spherical (Fig. 5B). Thus the timing and pattern of RhoGEF2 and Dia localisation together with the specific defects in furrow canal formation strongly suggest that RhoGEF2 and Dia have an instructive function for the pattern and mechanism of membrane invagination.

Dia localisation at the furrow canal depends on RhoGEF2, but not on F-actin

Dia, RhoGEF2 and F-actin localisation may functionally depend on each other. We first tested whether F-actin is required for the localisation of Dia and RhoGEF2 at the furrow canal by treating permeabilised embryos with the drug latrunculin A (Coue et al., 1987) to depolymerise F-actin (Fig. 6). We observed that the distribution of the actin binding protein moesin (Polescello and Payre, 2004) depends on the presence of actin filaments (Fig. 6C), whereas Dia and RhoGEF2 localisation was not affected by the latrunculin treatment (Fig. 6A,B). These data show that Dia and RhoGEF2 localise at the furrow canal independently of F-actin and thus may act upstream of F-actin polymerisation.

Second, we tested whether F-actin localisation at the furrow canal depends on *RhoGEF2* and *dia*, comparing phalloidin staining in wild-type, *RhoGEF2* and *dia* mutant embryos in the early phase of cellularisation and observed a consistent reduction of F-actin at the furrow canal in *RhoGEF2* embryos, which was even more prominent in embryos from *dia* germline clones (n>20, Fig. 7A-D). Consistent with the reduction of F-actin at the furrow canal, levels of MyoII were also reduced in the mutant embryos (see Fig. S3 in the supplementary material). In contrast to the reduction at the furrow canal, cortical F-actin appeared to be increased in some embryos from *dia* germline clones. This increase was variable and not observed in all of the experiments, however. These data suggest

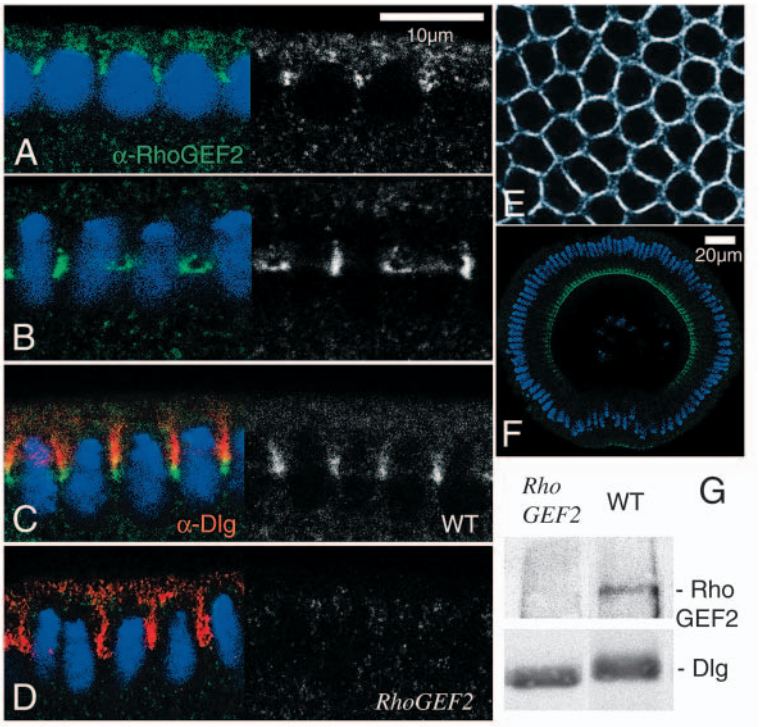

Fig. 4. RhoGEF2 is enriched at the furrow canal. Embryos (heatfixed) stained with RhoGEF2 antibody (green, white), Dlg (red) and DNA (blue). Right half of A-D shows only the RhoGEF2 staining. (A-C,E,F) Wild type, (D) from *RhoGEF2*^{04291} germline clone. (E) Surface view; wild type. (F) Cross section of an embryo undergoing ventral furrow formation. Scale bar: (A-E) 10 μm, (F) 20 μm. (G) Western blot for RhoGEF2 or Dlg of extracts from wild-type embryos and embryos from *RhoGEF2*^{04291} germline clones.

that *RhoGEF2* and *dia* are involved in controlling a subpopulation of actin filaments at the furrow canal.

In a third step we assayed whether Dia localisation depends on *RhoGEF2*. In contrast to the striking localisation of Dia in wild-type embryos (Fig. 7E, *n*=56), in embryos from *RhoGEF2* germline clones Dia staining was dispersed during the first phase of cellularisation when the nuclei are still spherical (Fig. 7F, *n*=48). Later Dia became weakly enriched at the furrow canal (data not shown). To exclude the possibility that *RhoGEF2* affects Dia protein levels, we compared the total amount of Dia protein in wild-type and *RhoGEF2* mutant embryos by western blotting. We detected comparable amounts of Dia protein in both extracts (Fig. 7G), suggesting that *RhoGEF2* does not affect the synthesis or stability but rather the intracellular distribution of Dia. In contrast, RhoGEF2 localisation at the furrow canal is normal in embryos from *dia* germline clones (see Fig. S4 in the supplementary material). Consistent with the double mutant analysis, RhoGEF2 and Dia localise normally in *nullo* mutants and Sry-α distribution is unchanged in embryos from *RhoGEF2* and *dia* germline clones when compared to wild-type embryos (see Fig. S4 in the supplementary material). These data support a model in which RhoGEF2 localises to the site of membrane invagination and then directly or indirectly recruits Dia to this site, which in turn nucleates actin filaments in the hexagonal pattern instructed by RhoGEF2.

Does the small GTPase Rho1 provide a link among RhoGEF2, Dia and F-actin?

The proposed biochemical activities of the guanyl nucleotide exchange factor RhoGEF2 and the formin Dia suggest that

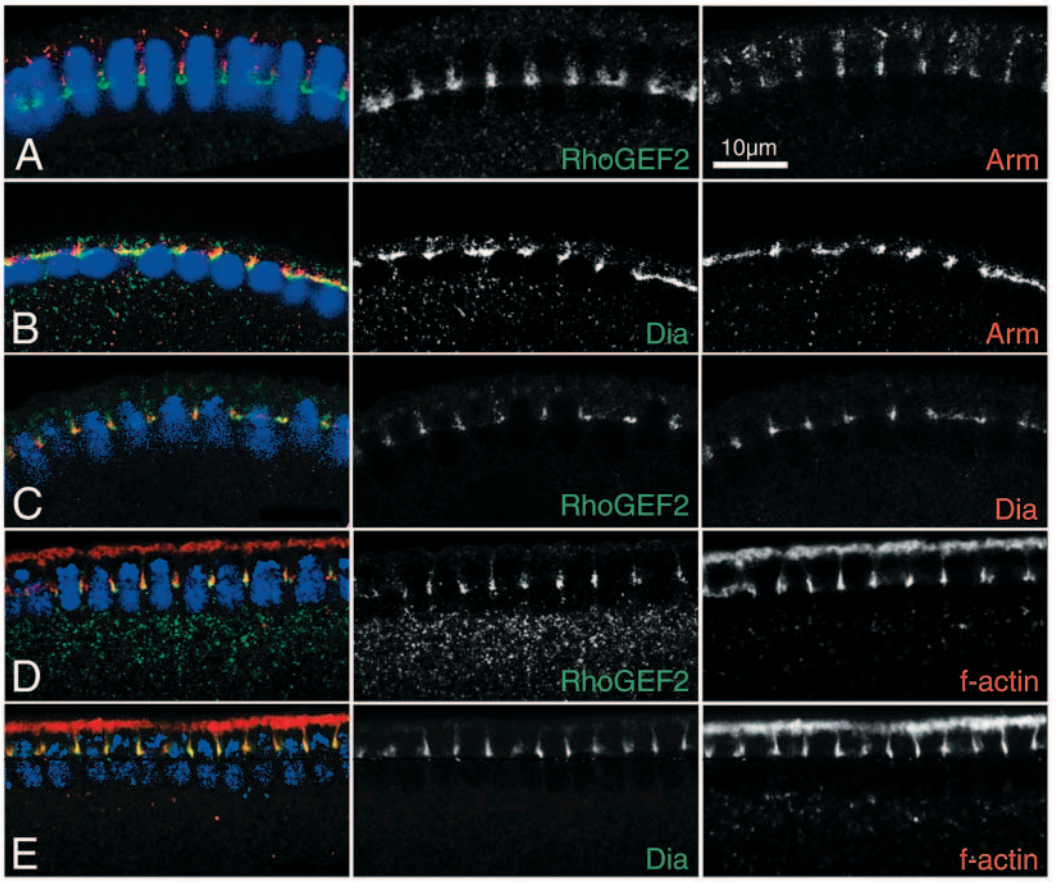

Fig. 5. RhoGEF2 colocalises with Dia and F-actin, but not Arm. Double labelling of wild-type embryos in green for (A,C,D) RhoGEF2, (B,E) Dia and in red for (A,B) Arm, (C) Dia and (E,F) F-actin. (A-C) heat-fixed, (D,E) fixed with formaldehyde. Scale bar: 10 μm.

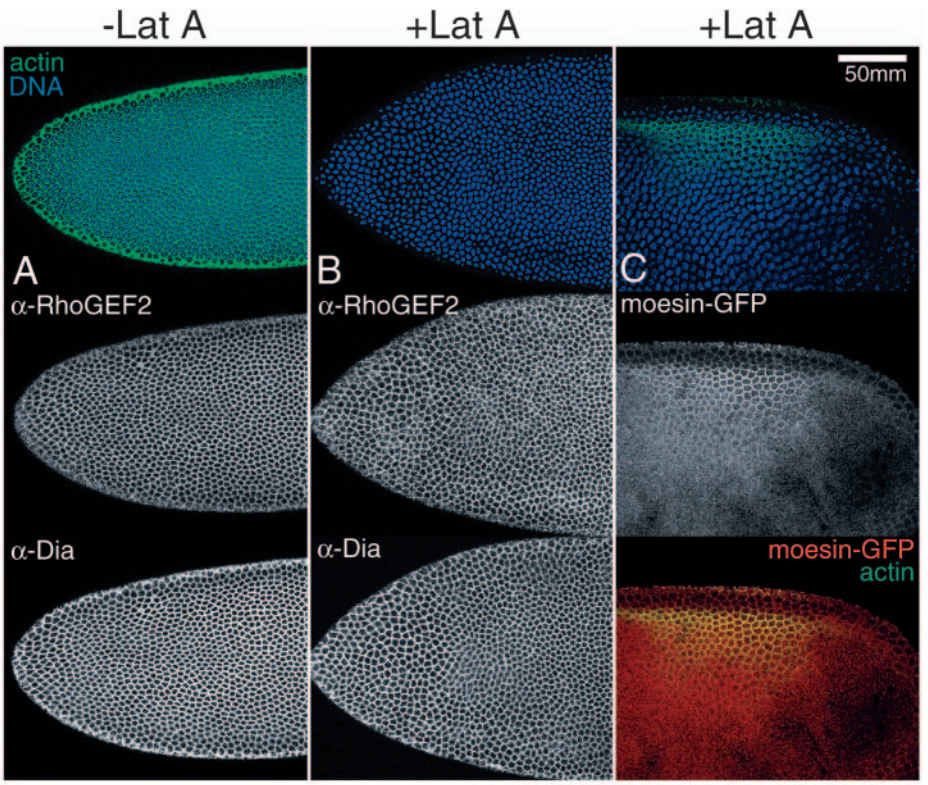

Fig. 6. RhoGEF2 and Dia localisation at the furrow canal do not depend on microfilaments. Permeabilized wild-type (A,B) embryos or (C) embryos with a GFP-moesin transgene were incubated with (A) buffer or (B,C) latrunculin A (LatA) to inhibit actin polymerisation, and stained for DNA (blue), F-actin (green); (A,B) RhoGEF2 and Dia; (C) GFP fluorescence. Scale bar: 50 μm.

RhoGEF2 activates a Rho type GTPase and that actin polymerisation by Dia is activated by a Rho type GTPase. To critically test such a model we reconstituted the interactions in vitro with purified components (see Fig. S5 in the supplementary material). First, to identify the substrates of the RhoGEF2 guanyl-nucleotide exchange activity we sampled all six *Drosophila* Rho GTPases (Newsome et al., 2000) in an in vitro GDP-GTP exchange assay (Fig. 8A,B). We loaded GST fusion proteins of Rho GTPases with ^{3}H-labelled GDP and measured the release of GDP catalysed by the GEF domain of RhoGEF2. We found that GDP was significantly released only from the Rho1 protein, but not from the RhoL, Rac or Cdc42 GTPases, whereas the GEF domain of Trio was specific for the three Rac GTPases (Newsome et al., 2000). The GEF domain of RhoGEF2 with a single point mutation (T1544A) (Zhu et al., 2000) and GST had no activity. Consistent with the reported genetic interaction of *RhoGEF2* and *Rho1* (Barrett et al., 1997), these data show that Rho1 is the only GEF substrate of RhoGEF2.

Second, we tested the physical interaction of Rho1 and Dia with an in vitro binding assay (Fig. 8C). We found GST-Rho1 bound to the N-terminal part of Dia (DiaΔC464), but not to a fragment of Dia lacking the putative Rho binding domain (DiaΔN318). The association of Rho1 and Dia was stronger with the activated form of Rho1 (Rho1Q63L) than with the GDP-loaded form.

In a third step, we tested whether Dia can induce actin polymerisation in a Rho1-dependent manner (Li and Higgs, 2003). We purified two fragments of Dia: an N-terminal fragment (DiaΔC518, containing the Rho-binding site) and a C-terminal fragment (DiaΔN519, containing the FH1, FH2 and autoinhibitory domains) and tested their activity on actin polymerisation in vitro. The C-terminal part alone induced actin polymerisation at submicromolar concentrations (see Fig. S6 in the supplementary material) similar to BNI1 fragments from yeast (Pruyne et al., 2002). This activity was inhibited by equimolar amounts of the N-terminal part, but was partially restored by a 10-fold molar excess of Rho1 (Fig. 8D). However, no difference in activity was observed between activated forms of Rho1 (loaded with GTPγS, GMP-PNP or Rho1Q63L) and Rho1 loaded with GDP (data not shown). Our data show that the C-terminal part of Dia is sufficient for efficiently polymerising actin filaments. The polymerisation activity is inhibited by the N-terminal part, suggesting that Dia activity is controlled by an intramolecular inhibition. However, since it was not possible to fully reconstitute the release of Dia autoinhibition by Rho1, a behaviour also described for mDia1 (Li and Higgs, 2003), the mechanisms for Dia activation remains elusive. Together with the weak binding of Rho and Dia that only slightly depended on the activation state of Rho1 and consistent with the properties of mDia1, these data indicate, that Rho1-independent mechanisms appear to be involved (Wallar and Alberts, 2003).

Discussion

Changes of cell shape and curvature of the plasma membrane depend on the reorganisation of actin filaments. During cellularisation, actin fibres are assembled in a hexagonal array that prefigures the invagination of the plasma membrane. We have presented evidence supporting the model that spatially restricted assembly of actin filaments by the formin Dia at the site of invagination is involved in bending the plasma membrane and in furrow canal formation. These actin filaments may form a coat that determines the shape and stability of the furrow canal.

Our morphological analysis of the mutant phenotypes reveals a new function of *RhoGEF2* and *dia* in the formation of the furrow canal. This function is consistent with the co-localisation of both proteins with F-actin at the furrow canal and the reduced amounts of F-actin in *RhoGEF2* and *dia* mutants. Biochemical analysis demonstrates actin polymerisation by Dia and thus supports the model that RhoGEF2 and Dia organise actin filaments to control the formation of the furrow canals. Furthermore, we provide evidence that the previously characterised genes *nullo* and *sry-*

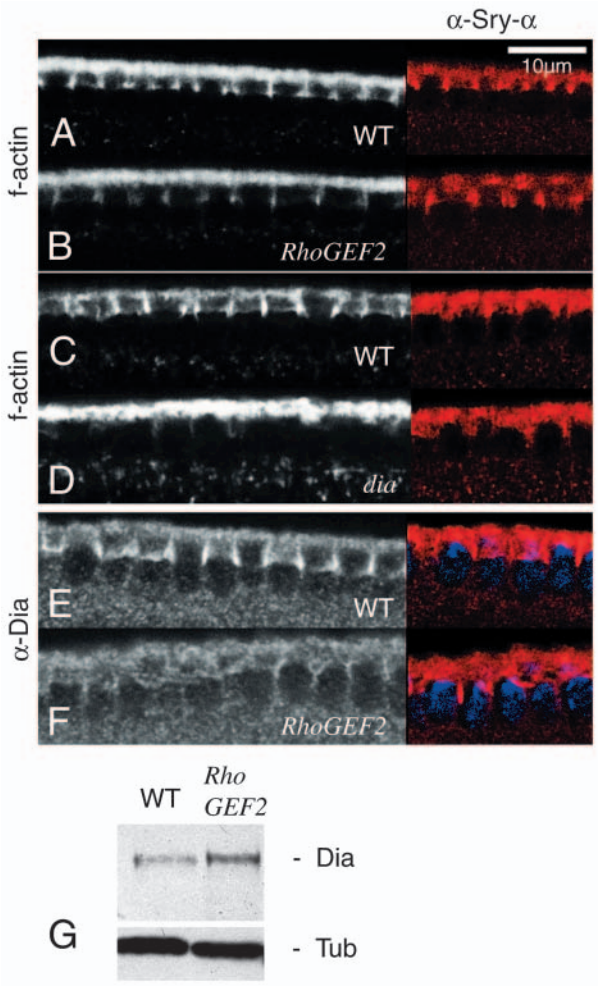

Fig. 7. F-actin and Dia localisation depend on *RhoGEF2*. (A,C,E) Wild-type embryos and embryos from (B,F) *RhoGEF2*$^{1.1}$ and (D) *dia* germline clones stained for (A-D) F-actin (left, white), (E,F) Dia (left, white), Sry-α (red) and DNA (blue). Sry-α staining indicates equal staining conditions. (G) Western blot for Dia and α-tubulin with extracts from wild-type, *RhoGEF2*$^{1.1}$ or *dia* germline clones embryos. Scale bar: 10 μm.

α act in a genetic pathway in parallel to *RhoGEF2* and *dia*, suggesting that they control two distinct aspects of furrow canal formation. This conclusion is based on the assumption that we used amorphic situtations in our experiment. We cannot exclude that *RhoGEF2* and *dia* stabilise the furrow canal rather than control its initial formation. A function in the formation is supported by our observation that the proportion of nuclei in multinuclear cells does not increase in the course of cellularisation.

The following arguments support the hypothesis that *RhoGEF2* and *dia* act in the same genetic pathway that controls spatially restricted assembly of actin filaments. In both *dia* and *RhoGEF2* mutants the morphology of the furrow canal is disrupted. The furrow canals are much larger than normal and filled with cytoplasmic blebs (Fig. 1). Both proteins are localised at the furrow canal and both precede the appearance of the cellularisation front (Fig. 5). The localisation of both proteins does not depend on F-actin (Fig. 6). However, they are directly or indirectly involved in the assembly of F-actin since the amount of F-actin is reduced at the furrow canal of the mutant embryos (Fig. 7). The strongest argument for a functional connection is that Dia localisation at the furrow canal depends on *RhoGEF2* during the early phase of cellularisation (Fig. 7). Rho1 may mediate this functional link by direct interactions with RhoGEF2 and Dia (Fig. 8). However, our findings do not show that *RhoGEF2* exclusively functions via *dia*. Other targets of Rho1-GTP, like citron kinase, protein kinase N or Rho kinase (Lu and Settleman, 1999b; Shandala et al., 2004; Naim et al., 2004; D'Avino et al., 2004; Royou et al., 2004) may be activated in parallel to Dia. Although we observe a reduction of MyoII at the furrow canal during the first half of cellularisation in embryos from *RhoGEF2* germline clones, correspondingly lower MyoII levels are also observed in embryos from *dia* germline clones, which indicates that the reduction of MyoII may be a consequence of reduced F-actin levels. Consistent with the reduction of F-actin at the furrow canal, levels of MyoII were also reduced in the mutant embryos (see Fig. S3 in the supplementary material). In contrast to the reduction at the furrow canal, cortical F-actin appeared to be increased in some embryos from *dia* germline clones. This increase was variable and not observed in all of the experiments, however.

The difference in the *RhoGEF2* and *dia* mutant phenotypes clearly shows that *dia* has additional functions and may be controlled by other not yet identified factors besides RhoGEF2. Whereas *RhoGEF2* mutants pass through the cleavage cycles without obvious defects (data not shown), *dia* is involved in formation of pole cells and pseudo cleavage furrows (Afshar et al., 2000). As a possible consequence of these additional functions, *dia* mutants in contrast to *RhoGEF2* mutants often have a more disrupted F-actin array, larger furrow canals and a more disturbed cellularisation than *RhoGEF2* mutants (Figs 1, 2). Furthermore in the early phase of cellularisation Dia localisation depends on *RhoGEF2*, whereas later, after the furrow has formed, Dia becomes enriched to a certain degree at the cellularisation front independently of *RhoGEF2*. One gene that may act in parallel to RhoGEF2 to control Dia localisation is *Abl*. Embryos from *Abl* germline clones have reduced amounts of Dia at the furrow canal and show a disrupted F-actin array similar to that observed in *dia* and *RhoGEF2* mutants (Grevengoed et al., 2003). However, the molecular link between Abl and Dia is elusive and no abnormalities in the morphology of the furrow canal in *Abl* mutants have been described. Thus Dia may be controlled and activated by multiple pathways including RhoGEF2 among others.

It is not known how the position of the invaginating plasma membrane is determined. RhoGEF2 and Dia are not likely to be part of a pattern formation process, but their localisation reflects an early readout of this pattern, since the nuclei and centrosomes are properly arranged in *RhoGEF2* and *dia* mutants (Fig. 2). RhoGEF2 and Dia proteins are early markers for these sites and precede furrow canal formation because we detected specific staining for both Dia and RhoGEF2 when the nuclei were still spherical and when the cellularisation front was not yet visible (Fig. 4A, Fig. 5B). Other factors beside RhoGEF2 and Dia are also involved in furrow canal formation, because many furrow canals still form in *RhoGEF2* and *dia* mutants, which indicates that there is genetic redundancy.

At present we can only speculate about which factors and

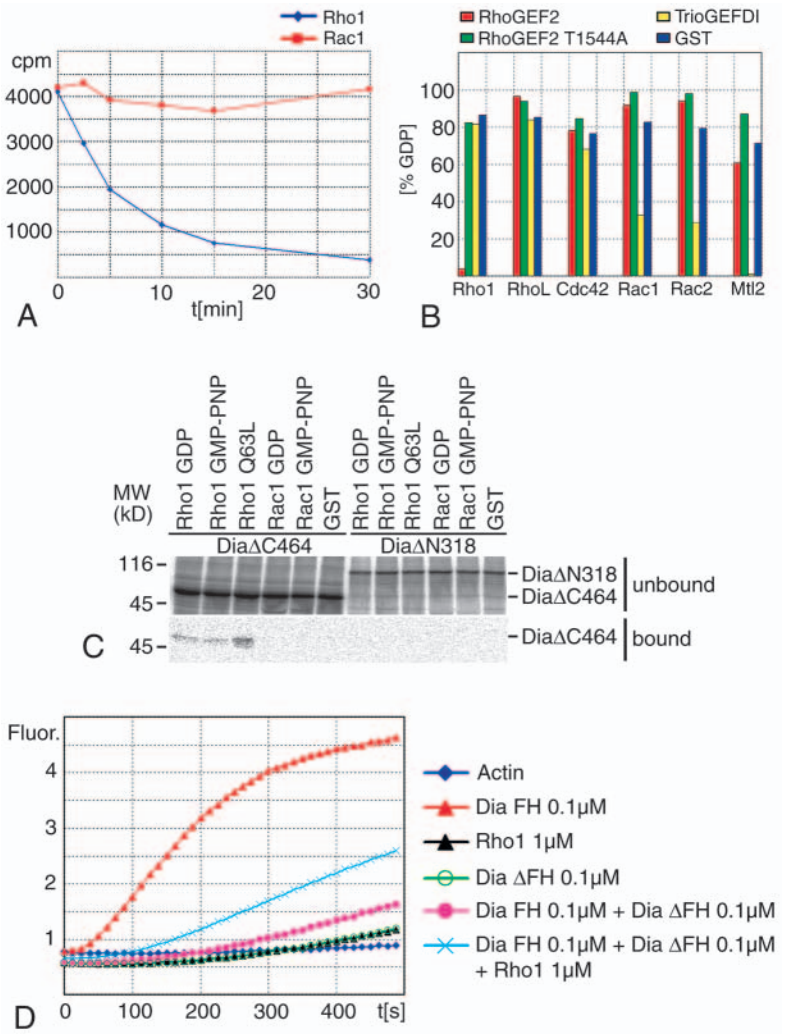

Fig. 8. Rho1 is a substrate of RhoGEF2 and binds and activates Dia. (A) Release of tritium-loaded GDP from Rho1 and Rac1 GST fusion proteins by a fusion protein of GST and the GEF domain from RhoGEF2. Bound GDP (expressed as counts of radioactivity per minute; cpm) plotted against incubation time. (B) Specificity of GDP release. Tritium loaded GST fusion proteins were incubated with GST fusion proteins of the GEF domains of RhoGEF2 and Trio (domain 1) or GST for 20 minutes. Bound GDP is indicated as the quotient of [GDP](t=0 minutes) and [GDP](t=20 minutes). The protein T1544A has a single point mutation in the GEF domain of RhoGEF2. (C) GST, GST-Rho1, GST-Rho1Q63L, GST-Rac1, (loaded with GDP or GMP-PNP) bound to glutathione Sepharose were incubated with reticulocyte lysate containing ^{35}S-labelled DiaΔN318 or DiaΔC464. Rho1Q63L has no GTPase activity. Bound and unbound fractions were analysed by SDS-PAGE and autoradiography. (D) Actin polymerisation induced by Dia. Time course of fluorescence (relative units) of pyrene-labelled actin (3 μM) and the indicated components. Dia FH, ZZ-DiaΔN519, Dia ΔFH, ZZ-DiaΔC518, Rho1, GST-Rho1 loaded with GTPγS. Rho1 loaded with GDP or GMP-PNP or Rho1Q63L released autoinhibition to a similar degree.

mechanisms are responsible for RhoGEF2 localisation. Candidates may be among the group of genes involved in furrow canal formation. However, for all of these mutations no ultrastructural analysis has been reported that would allow us to define the morphological defect and compare their function for furrow canal formation with the function of *RhoGEF2* and *dia*. Among this group are *Rab11* and *nuf*, which encode a GTPase of the recycling endosome and its putative effector (Riggs et al., 2003). Considering the assumed biochemical activities, it is conceivable that vesicle targeting is important for transporting factors to the site of membrane invagination (Riggs et al., 2003). This raises the possibility that RhoGEF2 is transported by such vesicles to the sites of membrane infolding. Analysis of RhoGEF2 protein distribution in *nuf* and *Rab11* mutants and the phenotype of double mutants may address this hypothesis. Alternatively, RhoGEF2 may be transported to the site of the future furrow canal along microtubules that form open baskets around the nuclei, or other recruiting factors may precede at the site of membrane invagination.

Furthermore, *slam* is required for timed formation of the furrow and invagination of the membrane in the first half of cellularisation. Like Dia and RhoGEF2 Slam protein localises to the furrow canal and localisation precedes furrow canal formation. Slam may act by recruiting MyoII to the furrow canal, but the biochemical activities of Slam have not been defined (Lecuit et al., 2002; Stein et al., 2002). Although the membrane does not invaginate initially in *slam* mutants, a complete F-actin array is visible (Fig. 2). Thus despite the overlapping localisation of Slam, RhoGEF2 and Dia their functions are clearly distinguishable.

How do RhoGEF2 and Dia act in furrow canal formation? If we consider the biochemical activity of Dia to nucleate actin filaments (Fig. 8) and the enlarged and labile furrow canals in the *dia* mutants (Fig. 1), it is conceivable that Dia organises and assembles a coat of F-actin at the site of membrane invagination and furrow canal formation. The coat of F-actin may be important for the compactness and stability of the furrow canal to prevent infoldings of the cytoplasm. Such a function may be related to the function of F-actin in endocytic events (Engqvist-Goldstein and Drubin, 2003). The subset of actin filaments controlled by *RhoGEF2* would not significantly contribute to pulling in the plasma membrane, since membrane invagination proceeds with normal speed in *RhoGEF2* mutants. Alternatively, RhoGEF2 and Dia may perform their function independently of actin polymerisation. Although we have shown that the amount of F-actin is reduced in the mutants (Fig. 7), we do not exclude the possibility that the polymerisation activity of Dia is not required for all or part of its function. Dia may also influence the organisation of microtubules, as interactions of mDia1 with microtubules and EB1, a microtubule-associated protein, have been described (Ishizaki et al., 2001; Palazzo et al., 2001; Wen et al., 2004).

The differences in protein localisation and mutant phenotypes of *RhoGEF2* and *nullo* suggest that they have distinct activities. In contrast to the frequently missing furrow canals in single mutants, their complete absence in embryos lacking both gene functions (Fig. 3) clearly implies, however, that their functions are redundant from a genetic point of view.

As proposed by Hunter and Wieschaus (Hunter and Wieschaus, 2000) the basal junction that tethers the two membranes of the furrow and that is located apically to the furrow canal is controlled by *nullo*, whereas our results show that *RhoGEF2* and *dia* are required for the formation of a compact and stable furrow canal. If one of the two pathways is disturbed, the furrow canal can still form, albeit with a lower and variable efficiency that depends on the conditions. For example the *nullo* phenotype is strongly temperature sensitive (Hunter et al., 2002). However, if both pathways are affected, furrow canals do not form at all. Future studies will resolve how the actin filaments are involved in bending the plasma membrane that leads to the furrow canal and will further demonstrate how RhoGEF2 protein is expressed in the hexagonal array to serve as a template for local actin polymerisation.

We thank members of the ZMBH laboratories for discussion and support; members of the Görlich laboratory, S. Schmidt (GEF assay), O. Fackler and S. Hannemann (actin assay) for advice; and R. Grosse for comments on the manuscript. We are grateful for materials, reagents or fly stocks from K. Barrett, B. Dickson, D. Görlich, U. Häcker, H. Higgs, R. Lehmann, G. Magie, B. Mechler, D. Montell, D. Kiehart, N. Perrimon, S. Schmidt, M. Seedorf, S. Wasserman, E. Wieschaus, the Drosophila stock center (Bloomington, USA) and Hybridoma Bank (Iowa, USA). We thank Y. Kussler-Schneider for technical assistance and S. Jakobs for antibody purification. N.V. is supported by the Boehringer Ingelheim Fonds, A.M. by the DFG and J.G.'s laboratory by the Emmy Noether programme of the Deutsche Forschungsgemeinschaft.

Supplementary material

Supplementary material for this article is available at
http://dev.biologists.org/cgi/content/full/132/5/1009/DC1

References

Afshar, K., Stuart, B. and Wasserman, S. A. (2000). Functional analysis of the Drosophila FH protein in early embryonic development. *Development* **127**, 1887-1897.

Alberts, A. S. (2001). Identification of a carboxyl-terminal diaphanous-related formin homology protein autoregulatory domain. *J. Biol. Chem.* **276**, 2824-2830.

Barrett, K., Leptin, M. and Settleman, J. (1997). The Rho GTPase and a putative RhoGEF mediate a signaling pathway for the cell shape changes in Drosophila gastrulation. *Cell* **9**, 905-915.

Debant, A., Serra-Pages, C., Seipel, K., O'Brien, S., Tang, M., Park, S. H. and Streuli, M. (1996). The multidomain protein Trio binds the LAR transmembrane tyrosine phosphatase, contains a protein kinase domain, and has separate Rac-specific and Rho-specific guanine nucleotide exchange factor domains. *Proc. Natl. Acad. Sci. USA* **93**, 5466-5471.

Castrillon, D. H. and Wasserman, S. A. (1994). Diaphanous is required for cytokinesis in Drosophila and shares domains of similarity with the products of the limb deformity gene. *Development* **120**, 3367-3377.

Coue, M., Brenner, S. L., Spector, I. and Korn, E. D. (1987). Inhibition of actin polymerisation by latrunculin A. *FEBS Lett.* **213**, 316-318.

D'Avino, P. P., Savoian, M. S. and Glover, D. M. (2004). Mutations in sticky lead to defective organization of the contractile ring during cytokinesis and are enhanced by Rho and suppressed by Rac. *J. Cell Biol.* **166**, 61-71.

Engqvist-Goldstein, A. E. Y. and Drubin, D. G. (2003). Actin assembly and endocytosis: from yeast to mammals. *Annu. Rev. Cell Dev. Biol.* **19**, 287-332.

Etienne-Manneville, S. and Hall, A. (2002). Rho GTPases in cell biology. *Nature* **420**, 629-635.

Foe, V. F., Odell, G. M. and Edgar, B. A. (1993). Mitosis and morphogenesis in the Drosophila embryo: point and counterpoint. In *The Development of Drosophila melanogaster* (ed. M. Bate and A. Martinez Arias), pp. 149-300. Cold Spring Harbor, NY: Cold Spring Harbor Laboratory Press.

Glotzer, M. (2001). Animal cell cytokinesis. *Annu. Rev. Cell Dev. Biol.* **17**, 351-86.

Grevengoed, E. E., Fox, D. T., Gates, J. and Peifer, M. (2003). Balancing different types of actin polymerization at distinct sites: roles for Abelson kinase and Enabled. *J. Cell Biol.* **22**, 1267-1279.

Häcker, U. and Perrimon, N. (1998). DRhoGEF2 encodes a member of the Dbl family of oncogenes and controls cell shape changes during gastrulation in Drosophila. *Genes Dev.* **12**, 274-284.

Higashida, C., Miyoshi, T., Fujita, A., Oceguera-Yanez, F., Monypenny, J., Andau, Y., Narumiya, S. and Watanabe, N. (2004). Actin polymerization-driven molecular movement of mDia1 in living cells. *Science* **303**, 2007-2010.

Hunter, C. and Wieschaus, E. (2000). Regulated expression of nullo is required for the formation of distinct apical and basal adherens junctions in the Drosophila blastoderm. *J. Cell Biol.* **150**, 391-401.

Hunter, C., Sung, P., Schejter, E. D. and Wieschaus, E. (2002). Conserved domains of the nullo protein required for cell-suface localization and formation of adherens junctions. *Mol. Biol. Cell* **13**, 146-157.

Ishizaki, T., Morishima, Y., Okamoto, M., Furuyashiki, T., Kato, T. and Narumiya, S. (2001). Coordination of microtubules and the actin cytoskeleton by the Rho effector mDia1. *Nat. Cell Biol.* **3**, 8-14.

Kiehart, D. P., Galbraith, C. G., Edwards, K. A., Rickoll, W. L. and Montague, R. A. (2000). Multiple forces contribute to cell sheet morphogenesis for dorsal closure in Drosophila. *J. Cell Biol.* **149**, 471-490.

Kobielak, A., Pasolli, H. A. and Fuchs, E. (2004). Mammalian formin-1 participates in adherans junctions and polymerization of linear actin cables. *Nat. Cell Biol.* **6**, 21-30.

Lecuit, T., Samanta, R. and Wieschaus, E. (2002). slam encodes a developmental regulator of polarised membrane growth during cleavage of the Drosophila embryo. *Dev. Cell* **2**, 425-436.

Li, F. and Higgs, H. N. (2003). The mouse formin mDia1 is a potent actin nucleation factor regulated by autoinhibition. *Curr. Biol.* **13**, 1335-1340.

Lu, Y. and Settleman, J. (1999). The role of Rho family GTPases in development: lessons from Drosophila melanogaster. *Mol. Cell Biol. Res. Com.* **1**, 87-94.

Lu, Y. and Settleman, J. (1999). The Drosophila Pkn protein kinase is a Rho/Rac effector target required for dorsal closure during embryogenesis. *Genes Dev.* **13**, 1168-1180.

Luschnig, S., Moussian, B., Krauss, J., Desjeux, I., Perkovic, J. and Nüsslein-Volhard, C. (2004). An F1 genetic screen for maternal-effect mutations affecting embryonic pattern formation in Drosophila melanogaster. *Genetics* **167**, 325-342.

Mazumdar, A. and Mazumdar, M. (2002). How one becomes many: blastoderm cellularization in Drosophila melanogaster. *BioEssays* **24**, 1012-1022.

Naim, V., Imarisio, S., di Cunto, F., Gatti, M. and Bonaccorsi, S. (2004). Drosophila citron kinase is required for the final steps of cytokinesis. *Mol. Biol. Cell* **15**, 5053-5063.

Newsome, T. P., Schmidt, S., Dietzl, G., Keleman, K., Asling, B., Debant, A. and Dickson, B. J. (2000). Trio combines with Dock to regulate Pak activity during photoreceptor axon pathfinding in Drosophila. *Cell* **101**, 283-294.

Palazzo, A. F., Cook, A. S., Alberts, A. S. and Gundersen. B. (2001). mDia mediates Rho-regulated formation and orientation of stable microtubules. *Nat. Cell Biol.* **3**, 723-729.

Polesello, C. and Payre, F. (2004). Small is beautiful: what flies tell us about ERM protein fucntion in development. *Trends Cell Biol.* **14**, 294-302.

Postner, M. A. and Wieschaus, E. F. (1994). The nullo protein is a component of the actin-myosin network that mediates cellularization in *Drosophila* embryos. *J. Cell Sci.* **107**, 1863-1873.

Pruyne, D., Evangelista, M., Yang, C., Bi, E., Zigmond, S., Bretscher, A. and Boone, C. (2002). Role of formins in actin assembly: nucleation and barbed-end association. *Science* **297**, 612-615.

Revenu, C., Athman, R., Robine, S. and Louvard, D. (2004). The co-workers of actin filaments: from cell structures to signals. *Nat. Rev. Mol. Cell. Biol.* **5**, 635-646.

Riggs, B., Rothwell, W., Mische, S., Hickson, G. R. X., Matheson, J., Hays, T. S., Gould, G. W. and Sullivan, W. (2003). Actin cytoskeleton remodeling during early Drosophila furrow formation requires recycling endosomal components Nuclear-fallout and Rab11. *J. Cell Biol.* **163**, 143-154.

Roberts, D. B. (1998). Drosophila*, A Practical Approach.* Oxford, UK: Oxford University Press.

Romero, S., le Clainche, C., Didry, D., Egile, C., Pantaloni, D. and Carlier,

M.-F. (2004). Formin is a processive motor that requires profilin to accelerate actin assembly and associated ATP hydrolysis. *Cell* **119**, 419-429.
Rothwell, W. R., Fogerty, P., Field, C. and Sullivan, W. (1998). Nuclear-fallout, a Drosophila protein that cycles from the cytoplasm to the centrosomes, regulates cortical microfilament organization. *Development* **125**, 1295-1303.
Royou, A., Field, C., Sisson, J. C., Sullivan, W. and Karess, R. (2004). Reassessing the role and dynamics of nonmuscle myosin II during furrow formation in early Drosophila embryos. *Mol. Biol. Cell* **15**, 838-850.
Sagot, I., Rodal, A. A., Moseley, J., Goode, B. L. and Pellman, D. (2002). An actin nucleation mechanism mediated by Bni1 and profilin. *Nat. Cell Biol*. **4**, 42-50.
Schejter, E. D. and Wieschaus, E. (1993). Functional elements of the cytoskeleton in the early Drosophila embryo. *Annu. Rev. Cell Biol.* **9**, 67-99.
Schweisguth, F., Lepesant, J.-A. and Vincent, A. (1990). The serendipity-alpha gene encodes a membrane-associated protein required for the cellularization of the Drosophila embryo. *Genes Dev*. **4**, 922-931.
Shandala, T., Gregory, S. L., Dalton, H. E., Smallhorn, M. and Saint, R. (2004). Citron kinase is an essential effector of the Pbl-activated Rho signalling pathway in *Drosophila melanogaster. Development* **131**, 5053-5063.
Shimada, A., Nyitrai, M., Vetter, I. R., Kuhlmann, D., Bugyi, B., Narumiva, S., Geeves, M. A. and Wittinghofer, A. (2004). The core FH2 doamin of diaphanous-related formins is an elongated actin binding protein that inhibits polymerisation. *Mol. Cell* **13**, 511-522.
Stein, J. A., Broihier, H. T., Moore, L. A. and Lehmann, R. (2002). Slow as molasses is required for polarized membrane growth and germ cell migration in *Drosophila*. *Development* **129**, 3925-3934.
Wallar, B. J. and Alberts, A. S. (2003). The formins: active scaffolds that remodel the cytoskeleton. *Trends Cell Biol.* **13**, 435-446.
Watanabe, N., Madaule, P., Reid, T., Ishizaki, T., Watanabe, G., Kakizuka, A., Saito, Y., Nakao, K., Jockusch, B. M. and Narumiya, S. (1997). p140mDia, a mammalian homolog of Drosophila diaphanous, is a target protein for Rho small GTPase and is a ligand for profilin. *EMBO J*. **16**, 3044-3056.
Watanabe, N., Kato, T., Fujita, A., Ishizaki, T. and Narumiya, S. (1999). Cooperation between mDia1 and ROCK in Rho-induced actin reorganization. *Nat. Cell Biol.* **1**, 136-143.
Wen, Y., Eng, C. H., Schmoranzer, J., Cabrera-Poch, N., Morris, E. J., Chen, M., Wallar, A. S., Alberts, A. S. and Gundersen, G. G. (2004). EB1 and APC bind to mDia to stabilize microtubules downstream of Rho and promote cell migration. *Nat. Cell Biol.* **6**, 820-830.
Xu, Y., Moseley, J. B., Sagot, I., Poy, F., Pellman, D., Goode, B. L. and Eck, M. J. (2004). Crystal structures of a formin homology-2 domain reveal a tethered dimer architecture. *Cell* **116**, 711-723.
Yasuda, S., Oceguera-Yanez, F., Kato, T., Okamoto, M., Yonemura, S., Terada, Y., Ishizaki, T. and Narumiya, S. (2004). Cdc42 and mDia3 regulate microtubule attachment to kinetochores. *Nature* **428**, 767-771.
Zhang, C. X., Lee, M. P., Chen, A. D., Brown, S. D. and Hsieh, T.-s. (1996). Isolation and characterization of a Drosophila gene essential for early embryonic development and formation of cortical cleavage furrows. *J. Cell Biol.* **134**, 923-934.
Zhu, K., Debreceni, B., Li, R. and Zheng, Y. (2000). Identification of Rho GTPase-dependent sites in the Dbl homology domain of oncogenic Dbl that are required for transformation. *J. Biol. Chem.* **275**, 25993-26001.